Enasidenib Induces Acute Myeloid Leukemia Cell Differentiation to Promote Clinical Response

Michael D. Amatangelo[1]*, Lynn Quek[2]*, Alan Shih[3]*, Eytan M. Stein[3], Mikhail Roshal[3], Muriel D. David[4], Benoit Marteyn[5], Noushin Rahnamay Farnoud[6], Stephane de Botton[7], Olivier A. Bernard[4], Bin Wu[8], Katharine E. Yen[8], Martin S. Tallman[3], Elli Papaemmanuil[6,9], Virginie Penard-Lacronique[4], Anjan Thakurta[1†], Paresh Vyas[2†], Ross L. Levine[3,6,10†]

***These authors contributed equally to this work and are co-lead authors**
†These authors contributed equally to this work and are co-senior authors

[1]Celgene Corporation, Summit, NJ, [2]Medical Research Council Molecular Hematology Unit, Oxford Comprehensive Biomedical Research Centre, Weatherall Institute of Molecular Medicine and Department of Hematology, Oxford University Hospital NHS Foundation Trust, Oxford, United Kingdom, University of Oxford, Oxford, United Kingdom, [3]Department of Medicine, Leukemia Service, Memorial Sloan Kettering Cancer Center, New York, NY, [4]Gustave Roussy, INSERM U1170, Université Paris-Saclay, 94805 Villejuif, France, [5]Unité de Pathogénie Microbienne Moléculaire, Institut Pasteur, Paris, France, [6]Center for Hematologic Malignancies, Memorial Sloan Kettering Cancer Center, New York, NY, [7]Hématologie Clinique, Gustave Roussy, Université Paris-Saclay, Villejuif, France, [8]Agios Pharmaceuticals, Inc., Cambridge, MA, [9]Center for Molecular Oncology and Department of Epidemiology and Biostatistics, Memorial Sloan Kettering Cancer Center, New York, NY, [10]Human Oncology and Pathogenesis Program, Memorial Sloan Kettering Cancer Center, New York, NY

Corresponding author:

Anjan Thakurta, Ph.D.
Translational Development
Celgene Corporation
556 Morris Ave
Summit, New Jersey, 07901
Phone: 908-673-9176
athakurta@celgene.com

Short title: Enasidenib induces cell differentiation in R/R AML

Word Count: 4184

Abstract Word Count: 244

Tables/Figures: 6

References: 33

Key Points:

- Enasidenib inhibits mIDH2 leading to leukemic cell differentiation with emergence of functional mIDH2 neutrophils in rrAML patients.
- RAS pathway mutations, and increased mutational burden overall, are associated with a decreased response rate to mIDH2 inhibition.

Abstract: Recurrent mutations at R140 and R172 in *isocitrate dehydrogenase 2* (*IDH2*) occur in many cancers, including ~12% of acute myeloid leukemia (AML). In preclinical models these mutations cause accumulation of the oncogenic metabolite R-2-hydroxyglutarate (2-HG) and induce hematopoietic differentiation block. Single-agent enasidenib (AG-221/CC-90007), a selective mutant IDH2 (mIDH2) inhibitor, produced an overall response rate of 40.3% in relapsed/refractory AML patients with *mIDH2* in a phase 1 trial. However, its mechanism of action and biomarkers associated with response remain unclear. Here, we measured 2-HG, *mIDH2* allele burden, and co-occurring somatic mutations in sequential patient samples from the clinical trial and correlated these with clinical response. Furthermore, we used flow cytometry to assess inhibition of mIDH2 on hematopoietic differentiation. We observed potent 2-HG suppression in both R140 and R172 m*IDH2* AML subtypes, with different kinetics, which preceded clinical response. Suppression of 2-HG alone did not predict response, as most non-responding patients also exhibited 2-HG suppression. Complete remission (CR) with persistence of m*IDH2* and normalization of hematopoietic stem and progenitor compartments with emergence of functional m*IDH2* neutrophils was observed. In a subset of CR patients, m*IDH2* allele burden was reduced and remained undetectable with response. Co-occurring mutations in *NRAS* and other MAPK pathway effectors were enriched in non-responding patients, consistent with RAS signaling contributing to primary therapeutic resistance. Together, these data support differentiation as the main mechanism of enasidenib efficacy in relapsed/refractory AML patients and provide insights into resistance mechanisms to inform future mechanism-based combination treatment studies.

Introduction

Somatic mutations in the *isocitrate dehydrogenase 2 (IDH2)* gene occur at conserved arginine residues (R140 and R172). These mutant proteins possess neomorphic enzymatic activity resulting in R-2-hydroxyglutarate accumulation.[1-4] R-2-HG competitively inhibits a set of alpha-ketoglutarate-dependent enzymes including the TET family of 5-methylcytosine (5mC) hydroxylases and the Jumonji-C domain histone demethylases.[5,6] This inhibition leads to DNA hypermethylation,[7] increased repressive histone methylation,[6] and impaired hematopoietic differentiation. Accordingly, inhibition of mutant IDH2 (mIDH2) reduces 2-HG levels and restores hematopoietic differentiation *in vitro*.[6,8-10]

Although both mutations are characterized by neomorphic enzymatic activity, myeloid malignancies with R140 and R172 IDH2 mutations are distinct with respect to clinical outcome, co-mutational profile, and molecular classification.[11-13] In preclinical studies, enasidenib (AG-221/CC-90007), a small-molecule inhibitor of mIDH2, reduced serum 2-HG, DNA hypermethylation, and repressive histone marks, and promoted hematopoietic differentiation in R140 and R172 mIDH2 models.[14-17] In a phase 1/2 clinical trial, enasidenib demonstrated clinical activity in patients with both R140 and R172 mIDH2 relapsed/refractory AML (rrAML) with an overall response rate (ORR) of 40.3%.[18] Here, we analyzed patient samples from this study to elucidate the mechanisms of action of enasidenib in R140 and R172 mIDH2 rrAML and to identify response biomarkers to targeted mIDH2 therapy.

Materials and Methods

Study Participants and Treatment

Analyses were performed on rrAML patient samples collected from the AG-221-C-001 study with informed consent. Patients were included in the AG-221-C-001 trial and in the translational studies here based on *IDH2* mutations detected by local testing. A retrospective central in vitro diagnostic test confirmed mutation status with a concordance rate above 95%. Enasidenib was administered to patients as described in the approved study protocol. Patient sample disposition indicating samples analyzed in each assay is supplied in **Figure S1**. Patient baseline characteristics and clinical responses of subpopulations analyzed vs the rrAML cohort as a whole are supplied in **Table S1**. Outcome data reflect an April 15th 2016 study cut-off date.

Measurement and Analysis of 2-hydroxyglutarate (2-HG)

Serum samples were collected from patients at screening within 28 days before the first dose of enasidenib and/or pre-dose on day 1 of each treatment cycle. 2-HG concentration was determined using liquid chromatography tandem mass spectrometry by Covance, Inc (formerly Tandem Labs) according to an analytically validated method. Baseline total 2-HG was determined to be either the average of the screening sample and the pre-dose cycle 1 sample, or either sample if both were not available. Maximum suppression of 2-HG levels was determined by comparing the lowest level of 2-HG observed on-treatment to baseline 2-HG level. Time to maximum suppression was the first time point where 2-HG level was within 5% of maximum suppression for that patient.

Sysmex OncoBeam^{TM} Digital Polymerase Chain Reaction

Bone marrow and/or peripheral blood samples were collected at screening 28 days before the first dose of enasidenib and during treatment and processed to peripheral blood mononuclear cells (PBMC) and bone marrow mononuclear cells (BMMCs). Measurement of mutant and wild

type *IDH2* was determined using Sysmex BEAMing technology. Briefly, DNA was extracted from samples, pre-amplified in a multiplex PCR reaction and amplified with nested primers in an emulsion PCR reaction on the surface of magnetic beads in water–in-oil emulsions. Fluorescently labeled probes specific to the *IDH2* mutation and to the wild-type sequence were hybridized to the uncovered DNA fragments on the bead surface. Fluorescently labeled beads were quantified using flow cytometry.

Blast Percentage Determination by Flow and mIDH2 Assessment

Multi-parameter flow cytometry was performed on bone marrow aspirates at diagnosis and at day 1 of each treatment cycle. Abnormal populations were identified by antigen expression as described previously.[19,20] Briefly, up to 1.5 million cells from freshly drawn bone marrow aspirate were stained with three ten-"color" panels (**Table S2**), washed and acquired on a FACS-Canto-10 cytometer (BD Biosciences, San Jose CA). The results were analyzed using custom Woodlist software (generous gift of Wood BL, University of Washington). Following flow assessment, samples were lysed and assessed for m*IDH2* as part a 28-gene amplicon capture-based next generation sequencing (NGS) assay at Memorial Sloan Kettering Cancer Center.

Hematopoietic Immunophenotyping and mIDH2 Assessment in Flow-Sorted Cells

Viably-frozen BMMCs from normal donors (N=12) or refractory/relapsed rrAML patients (N=9) were thawed, stained with antibodies listed in **Table S3** and sorted on either a BD LSR Fortessa or BD FACSAria Fusion (Becton Dickinson, Oxford UK). Sorted fractions (> 95% purity) of lin-ve CD34-CD117- cells, which represent mature myelomonocytic cells, and unsorted mononuclear cells were processed for genomic DNA (gDNA). Whole genome amplification (WGA, RepliG, Qiagen UK) was carried out in samples with less than 10^4 cells or where extracted gDNA was inadequate. Analyses of m*IDH2* at R140 and R172 codons were completed by PCR of exon 4 of the *IDH2* gene followed by NGS using a MiSeq (Illumina, UK).

Phagocytosis Assay

Neutrophils were collected from fresh citrated blood by centrifugation, red blood cell sedimentation, and Percoll gradient cell separation. Purified neutrophils (1×10^6) were incubated with 3 µL fluorescent green latex beads (Sigma, France) for 15 minutes at 37°C in 1 mL RPMI medium supplemented with 10% heat-inactivated fetal bovine serum (Sigma). Cells were washed, fixed in 3.3% paraformaldehyde, stained with DAPI and imaged with a laser-scanning TCS SP5 confocal microscope (Leica, France). The percentage of neutrophils containing latex beads was calculated by scoring 5 different fields of view for each sample. *IDH2* mutations were confirmed in neutrophils with a TaqMan® SNP Genotyping Assay (Life Technologies, Carlsbad CA).

FoundationOne Heme Panel

FoundationOne® Heme analysis was conducted in a clinical laboratory improvement amendments (CLIA)-certified lab by Foundation Medicine, Inc. Briefly, fresh bone marrow and/or peripheral blood samples were collected from patients and DNA and RNA were extracted. Nucleic acid libraries were prepared, captured using custom bait-sets and sequenced to high depth using Illumina HiSeq for 405 cancer-related genes by DNA-sequencing (DNA-seq) and 265 frequently rearranged genes by RNA-sequencing (RNA-seq). Only known or likely gene mutations that are the targets of therapies, either approved or in clinical trials, or are otherwise known drivers of oncogenesis published in the literature were included in this analysis.[21] Co-mutational burden was calculated as the total sum of all unique known and likely somatic mutations, other than *IDH2*, identified in each patient.

Calculation of Variant Allele Frequency (VAF)

In each assay VAF was calculated as measurement of mutated allele (i.e., m*IDH2*) over measurement of mutated allele + wild type allele (i.e., *mIDH2* + wild type *IDH2*) in each sample.

Statistical Analysis

Statistical analyses were performed with GraphPad Prism software using methods noted in figure and table legends. Mutational associations with either overall response rate (ORR) or complete remission (CR) rate were assessed through a two-tailed Fisher's Exact test on a 2 x 2 contingency table analyzing the sum of patients achieving a response or not (ORR ≥ partial remission [PR]; and CR ≥ morphologic leukemia-free state [MLFS]) vs presence or absence of gene mutation identified by FoundationOne® Heme. Associations between prognostic risk groups and response were assessed using a two-tailed Chi-square test for trend on a 3 x 2 contingency table analyzing the sum of patients achieving a response or not (ORR ≥ PR; CR = CR) vs risk classification as favorable, intermediate or adverse as stated in figure legends.

Results

mIDH2 Inhibition Is Associated with Potent Reduction of 2-HG in mIDH2 AML

Total 2-HG measurements in blood correlate with R-2-HG levels, tumor mass, clinical response to cytotoxic therapy and are a proposed a biomarker of IDH2 mutations.[4] Therefore, we assessed total 2-HG levels in 125 rrAML patients with available samples prior to enasidenib treatment and every 28 days during therapy. Median 2-HG suppression (defined as the maximum extent of suppression compared to pre-therapy) was 90.6%, consistent with potent target inhibition. 2-HG suppression in patients with R172 mIDH2 was less than in patients with R140 mIDH2 rrAML (median suppression of 70.9% and 94.9%, respectively [$p < 0.001$]); consistent with preclinical data and an interim analysis of samples from study AG-221-C-001 (**Figure 1A**).[14-16,22-24] Of note, 5 patients during treatment had an increase in 2-HG. Two of these patients achieved a best response of PR despite never having 2-HG levels below baseline in multiple samples analyzed. None of these patients were observed to have co-occurring mutations in *IDH1*.

We next assessed 2-HG suppression in patients dosed with <100mg, 100mg, or >100mg enasidenib daily. Although we observed a trend towards greater 2-HG suppression at higher doses in R140 mIDH2 patients, there were no statistical differences in maximal 2-HG suppression among the three dosing groups ($p = 0.054$ for <100mg vs 100mg and $p = 0.094$ for 100mg vs >100mg) (**Figure 1B**). In R172 mIDH2 patients, 2-HG suppression was more variable across dosing groups (95% CI: 43.9%-102.9%, 10.7%-61.0% and 62.5%- 82.7% in the <100mg, 100mg, and >100mg dosing groups, respectively). A statistical difference in 2-HG suppression was observed between 100mg and >100mg dosing cohorts. However, the 100mg group was confounded by 4 patients whose 2-HG levels increased and no statistical difference was found in 2-HG suppression between <100mg vs >100mg dosing groups ($p = 0.152$ for <100mg vs 100mg, $p = 0.022$ for 100mg vs >100mg and $p = 0.955$ for <100mg vs >100mg). Furthermore, response rates for R172 mIDH2 patients were not statistically different between the 100mg and >100mg

dose groups analyzed (ORR 44.0% and 58.8%, respectively, p = 0.530, Fisher's exact test), suggesting no additional clinical benefit for R172 mIDH2 patients in dosing above 100mg. Importantly, no difference in time to maximum 2-HG suppression between patients dosed with <100mg, 100mg, or >100mg enasidenib daily was observed either (**Figure S2A**). Together, 2-HG suppression and efficacy data indicate that the 100mg enasidenib dose is biologically and therapeutically active in rrAML patients with m*IDH2*, regardless of the specific mutation.

We next assessed the relationship between pre-enasidenib therapy 2-HG levels and clinical response. We observed no significant difference in baseline 2-HG levels between patients achieving a CR, patients obtaining any response (R = CR with incomplete hematologic recovery [CRi], CR with incomplete platelet count recovery [CRp], MLFS, or PR) and patients who did not respond (NR = stable disease or progressive disease) (**Figure 1C**). We assessed whether timing of pharmacodynamic response, defined as maximal 2-HG suppression, correlated to best clinical response. Although the mean cycle number to maximal 2-HG suppression, best response (BR), and CR was ~1 treatment cycle later in R172 vs R140 patients (3 vs 2 cycles for maximal 2-HG suppression and BR, and 6 vs 5 cycles for CR) (**Figure 1D**), the ORR and CR rates for patients with R172 and R140 mutations were not statistically different.[18] These data demonstrate the kinetics of target 2-HG inhibition parallel the kinetics of clinical response without effect on response attainment.

Clinical Responses to mIDH2 Inhibition Do Not Correlate with mIDH2 Allele Burden

We evaluated whether m*IDH2* allele burden at baseline or changes on-therapy correlated with response to enasidenib by quantification of m*IDH2* VAF on unsorted samples using digital PCR and NGS. We observed a significant correlation between digital PCR and NGS for 45 matched patient samples run on both assays ($R^2 = 0.59$, $p < 0.0001$) (**Figure S2B**). A positive correlation trend was also observed between m*IDH2* VAF and 2-HG levels at screening in 17 patients with available samples, however, it was not statistically significant ($R^2 = 0.21$, $p = 0.0636$) (Figure S2C).

Notably, m*IDH2* allele burden was highly heterogeneous at screening among patients, ranging from low-level mutant positivity to fully clonal (~50%) (**Figure 2A and Figure S3A**). No association between *mIDH2* VAF at screening and clinical response was observed, and patients achieving CR had both low and high m*IDH2* burden. To assess the possibility that ancestral (clonal) and non-ancestral (subclonal) m*IDH2* disease exhibit different responses, we analyzed the VAF of co-occurring mutations in the 30 patients with low m*IDH2* VAF (< 0.2). Eight of these patients, 5 responders and 3 non-responders, had co-occurring mutations with VAF > 0.4, consistent with m*IDH2* occurring as a non-ancestral event (**Figure S4**). Taken together with data showing responses in both clonal and subclonal m*IDH2,* these data suggest that patients with ancestral or non-ancestral m*IDH2* clones can respond to enasidenib.

Next, we analyzed changes in absolute m*IDH2* VAF from screening to best response. A decrease in m*IDH2* VAF was more commonly observed in responding patients than an increase, however, only one-half of the patients showed a VAF change of more than 5% points (**Figure 2B and Figure S3B-C**). Similar to recent results reported for a subset of m*IDH1* AML patients treated with an mIDH1 inhibitor, longitudinal analysis by digital PCR in our cohort identified 9/29 CR patients for whom m*IDH2* became undetectable with enasidenib treatment.[25] Interestingly, all 9 patients had R140 m*IDH2* rrAML (50% of the 18 R140 CR patients) and loss of both a minor m*IDH2* subclone and a more substantive *mIDH2* clone (~40%) were observed. In 8 of these patients, m*IDH2* remained undetectable with continued treatment, consistent with persistent molecular remission (**Figure 2C**). However, no significant difference was observed in an initial analysis of event-free survival between patients achieving molecular remission vs patients achieving CR without molecular remission (295.9 vs 259.9 days, respectively, p = 0.784; event-free survival was defined according to protocol as the interval from date of first dose to date of documented relapse, progression, or death due to any cause, whichever occurred first). Finally, we assessed the relationship between two measures of leukemic burden: bone marrow blast count (flow

cytometry) and m*IDH2* VAF (genetic) in 9 additional patients who responded to enasidenib (**Figure 2D**). In 6 of these patients, we observed marked blast count decreases to near 0% in aspirates with concomitant m*IDH2* VAF above 10%. This data demonstrates that m*IDH2* cells persist in most patients achieving CR and a reduction in m*IDH2* allele burden during treatment is neither necessary nor sufficient for clinical response to enasidenib.

Clinical Response to mIDH2 Inhibition Is Associated with Induction of Myeloid Differentiation

Given that a reduction in m*IDH2* VAF was not required for CR, we hypothesized that enasidenib might induce clinical response by promoting leukemic cell differentiation. We measured the magnitude of different immunophenotypic compartments in the hematopoietic hierarchy, before and during treatment, in 5 m*IDH2* rrAML patients who achieved CR or PR (**Figure 3A-B**). Prior to treatment, all 5 patients had expanded myeloid leukemic progenitor or precursor populations. Enasidenib treatment resulted in near normalization of the immature-to-mature cell population ratio at CR and PR in patients with both R140 (201-023 and 203-002) and R172 (104-036, 201-010 and 201-011) mIDH2. In contrast, no improvement of immature-to-mature ratio was observed in 5 non-responding patients (**Figure S5**). In the responding patients, we assayed m*IDH2* VAF by NGS in bulk BMMC and flow-sorted mature myeloid cells **(Figure 3B**). In 4 of 5 patients achieving CR or PR, m*IDH2* VAF remained stable (201-010, 201-011, 104-036) or increased (201-023) in both cell populations.

We extended these findings by measuring m*IDH2* VAF in peripheral blood neutrophils prior to enasidenib treatment and at the time of CR in 7 additional patients who achieved CR (**Figure 3C,** top panel). In 6 of 7 cases, m*IDH2* VAF remained constant between pre-therapy leukemic cells and neutrophils at CR, consistent with differentiation of m*IDH2* leukemia cells into mature neutrophils. Furthermore, in patient 104-018, the VAF of additional co-associated AML mutations remained unchanged in neutrophils at CR, consistent with enasidenib-mediated differentiation of a transformed leukemic clone (**Figure 3C,** middle panel). In contrast, in the 1 patient whose

m*IDH2* VAF dropped to 0% in mature neutrophils at CR (104-010), the VAF of other AML-associated mutations showed heterogeneous changes consistent with clonal selection rather than loss of all clonally derived leukemic cells (**Figure 3C,** top and bottom panels). Next, we investigated the functional status of differentiated leukemic neutrophils with m*IDH2* in 3 patients who achieved CR (**Table S4**). In each case, mutant neutrophils demonstrated intact phagocytic activity consistent with restoration of normal granulocyte function (**Figure 3D**)**.**

Genomic Predictors of Response to mIDH2 Inhibition

We assessed whether additional somatic mutations were associated with differential response by performing capture-based NGS with FoundationOne® Heme mutational panel in 100 patients at screening. No overt biases in response, age, sex, prior treatments, bone marrow blast percentage, absolute neutrophil counts, or prior myelodysplastic syndrome diagnosis were observed between these patients and the 176 rrAML patients from the phase 1 portion of study AG-221-C-001 (**Table S1**). Ninety-eight percent of samples contained mutations other than m*IDH2* and 17 co-occurring mutated genes were identified in ≥5% of patients (**Figure 4A-B**). The most frequent co-occurring mutations were in *SRSF2* (45%), *DNMT3A* (42%), *ASXL1* (27%), *RUNX1* (24%), *NRAS* (17%), and *BCOR* (15%). Notably, the prevalence of mutations in this cohort differed from an analysis of 1376 de novo AML samples from Papaemmanuil, et al (**Figure S6A-B**).[13] Our cohort included a significant enrichment of adverse risk mutations (*DNMT3A*, *ASXL1*, *RUNX1*). Statistical significance of *ASXL1* and *RUNX1* enrichment was also upheld when restricted to the 130 m*IDH2* positive patients in the Papaemmanuil dataset.[13] A significantly lower level of favorable prognosis mutations (*NPM1),* as defined by *Grimwade, et al,* were also observed.[26] Differences in co-occurring mutations in patients with R140 m*IDH2* AML, including increased co-mutational heterogeneity (60 different mutated genes vs 24 in R172 mIDH2 patients) and number of co-occurring mutations per patient (3.6 vs 2.6 mutations per patient in R172 m*IDH2*, p = 0.020) were observed (**Figure 4A and Figure S6C-E**). Additionally, some mutated

genes were either exclusively observed (*SRSF2*, n = 45) or more prevalent in R140 m*IDH2* rrAML (*RUNX1*, 27.3% vs 14.3% in R172 m*IDH2* rrAML) or more prevalent in R172 m*IDH2* rrAML (*DNMT3A*, 66.7% vs 36.4% in R140 m*IDH2*). This data extends work on *de novo* AML by showing that R140 and R172 m*IDH2* rrAML are genetically distinct leukemia subtypes.[13]

Additionally, cytogenetics were overlaid with mutational data to characterize the cohort by four different risk classifications of *de novo* AML.[13,26-28] Using the European LeukemiaNet classification from 2010, 14% of patients were classified as favorable risk and 59% were classified as intermediate risk (**Figure 4C**).[27,29] Using the recently revised ELN classification from 2017, which includes *ASXL1* and *RUNX1* mutations in the adverse risk group, a disproportionally large group of patients (56%) were classified as adverse risk.[28] Furthermore a classification scheme by Grimwade et al, which includes *DNMT3A* mutations in the adverse risk group, showed an even greater enrichment of adverse risk patients (73%).[26] Finally, a classifier developed on the *de novo* AML cohort[13] revealed an enrichment of patients with mutations in splicing/chromatin associated genes (43%), and with *TP53* mutations or aneuploidy (29%). Only 14% of patients were categorized as *NPM1* mutation-associated AML, which has been reported as the largest AML subset (**Figure 4D**). Importantly, clinical responses to enasidenib were observed across the risk spectrum in the 72 efficacy-evaluable patients with full genomic/cytogenetic data (**Table 1**).

Finally, we investigated whether the number of co-occurring mutations or specific mutant alleles correlated with enasidenib response. Patients who achieved a response (≥PR or CR) had significantly fewer co-occurring mutations than non-responders ($p < 0.001$, **Figure 5A**). Segregating patients in three tertiles (≤ 3, 3 to 6, and ≥ 6 co-mutations) revealed a significant difference in ORR for patients with the most vs least co-occurring mutations (ORR 21.9% vs 70.4%, respectively, $p < 0.001$) (**Figure 5B**). Analysis of co-mutated genes with response indicated a lower, but statistically non-significant, ORR with co-occurring *SRSF2* (34%), *ASXL1* (39%), *RUNX1* (26%), and *NRAS* (19%) mutations (**Table S5**)**.** However, significantly fewer

patients with co-occurring *NRAS* mutations achieved CR (p = 0.0114; **Table S5**). When the most common mutations known to activate NRAS signaling (G12, G13, or Q61) were analyzed vs ORR, the observed decrease in response rate was statistically significant (p = 0.002**, Figure 5C**). Notably, overall mutational burden was significantly higher (p < 0.001) in patients with m*NRAS* (G12, G13, or Q61) and mutations in *NRAS* were frequently subclonal (**Figure 5D-E**). Analysis of other gene mutations involved in activating MAPK signaling revealed that no patients with m*PTPN11* responded and m*KRAS* was not associated with response (**Table S5**). Together these data suggest that some RAS pathway mutations, either in the dominant or minor subclone, may directly or indirectly attenuate responses to mIDH2 inhibition.

Discussion

Our study of m*IDH2* rrAML patient samples from the phase 1 trial of enasidenib indicates that this cohort is enriched for mutations more commonly seen in adverse-risk or secondary AML (e.g., *SRSF2*, *RUNX1,* and *ASXL1)*. Additionally, these studies extend previous observations in *de novo* R140 and R172 *mIDH2* AML, confirming that the two *mIDH2* subtypes are genetically distinct. Despite these observations, enasidenib exhibited potent target inhibition in both subtypes and an ORR of ~40% with no statistical difference between R140 and R172 m*IDH2* rrAML.[18] Additionally, our data confirms the preclinical mechanism of action of m*IDH2* inhibition by enasidenib and provides the first insight into the genetic basis of primary resistance.[10,14-16]

Evidence suggests that human AML is composed of a hierarchy of both tumor-propagating leukemic stem cells (LSCs) arrested at a progenitor or precursor stage of hemopoiesis and more mature non-tumor propagating leukemic cells.[30,31] Our observations demonstrate enasidenib promotes terminal differentiation of m*IDH2* leukemic cells of granulocytic lineage in patients who achieve CR or PR. Furthermore, we observed *ex-vivo* phagocytic function in differentiated m*IDH2*-containing neutrophils. These observations are clinically important and may explain the lower frequency of infections in patients achieving CR with enasidenib treatment.[32] Our studies also demonstrate decreases in m*IDH2* below a detectable limit in a subgroup of patients. Both observations support differentiation as the mechanism of action of enasidenib monotherapy. Where m*IDH2* cells persist, it's most plausible that m*IDH2* LSCs are not eradicated but differentiate to give rise to m*IDH2*-containing functional neutrophils. When molecular CR is achieved, m*IDH2* inhibition may result in terminal or near terminal exhaustion through differentiation of the m*IDH2* clone. The differential effects may be due to the specific cellular and genetic contexts of the *IDH2* mutation and additional work will be required to dissect the mechanisms accounting for these observations. It is also intriguing and unclear how CR is

achieved in the context of subclonal *mIDH2*; this requires further mechanistic studies of cell autonomous and cell non-autonomous effects of *IDH2* mutations in AML.

In this study, we measured 2-HG, which includes both L-2-HG and R-2-HG, whereas only R-2-HG is produced by neomorphic IDH mutations. It has been shown that total 2-HG levels correlate with R-2-HG, m*IDH2* allelic burden, tumor mass and clinical status (i.e., CR vs absence of CR), consistent with the majority of 2-HG being derived from mIDH2 production of R-2-HG.[4] When 2-HG levels are low, measurement of R-2-HG, rather than total 2-HG, may improve sensitivity, however, this would not have changed our observations relating to the consistent, dose-dependent suppression of 2-HG seen in nearly all patients. Previously, serum 2-HG levels have been suggested as a biomarker for chemotherapy response in m*IDH2* positive patients.[1-4] Our data demonstrates this is not the case in targeted therapy because enasidenib is able to inhibit the mIDH2 enzyme and suppress 2-HG regardless of clinical response. Consistent with this hypothesis the level of suppression of 2-HG is not prognostic of response. We also observed that in R172 m*IDH2* patients, though the extent of 2-HG suppression is more variable and maximal suppression takes longer to achieve, clinical responses were equivalent to the R140 m*IDH2* subtype. Paradoxically, in 4 R172 patients, 2-HG levels rose on enasidenib therapy. This anomaly could arise from differential production of 2-HG by different cell populations during enasidenib-induced differentiation, specific co-mutational patterns, or alterations in AML cell metabolism in these patients not seen in the larger cohort. Taken together, these data demonstrate enasidenib potently suppresses 2-HG, the extent of 2-HG suppression does not predict clinical response, and primary resistance to enasidenib is not due to an inability to suppress mIDH2 enzyme activity.

These data also suggest other factors determine clinical response to enasidenib. Patients with a higher mutational burden and/or co-occurring mutations in the RAS pathway were observed to be less likely to respond to mIDH2 inhibition. The observation that increasing number of driver mutations is associated with poorer outcome with m*IDH2* inhibitor therapy mirrors similar

observations in newly diagnosed AML patients treated with chemotherapy.[13] From this data, it is unclear if constitutive activation of the RAS pathway imposes a 2-HG-independent differentiation block or whether mutations in *RAS* and other signaling pathways are a marker of overall higher mutational burden and other mechanisms of 2-HG-independent differentiation arrest. Notably, *NRAS* mutations were frequently present in a minor subclone and this intriguing observation requires further investigation.

Although enasidenib responses are clinically durable, the genetic heterogeneity observed in our patients suggests combination with other therapies may be required to achieve long-term disease remission in more patients. This is reminiscent of the impressive, but not durable, activity of ATRA monotherapy in acute promyelocytic leukemia.[33] Our data now suggests that targeted therapies may optimally be delivered in combination with other therapies. Current clinical studies combining enasidenib with combination chemotherapy or azacitidine, (NCT02677922 and NCT02632708) and future orthogonal targeted therapies will address this question. While this is only a subgroup analysis of a large single-arm experience, taken together, the clinical response and translational data demonstrate that single-agent mIDH2 inhibition by enasidenib in rrAML represents a critical and novel differentiation therapy. It also provides the platform for future combination therapy regimens to optimize clinical response and further improve outcomes in m*IDH2* AML.

Acknowledgments: Authors acknowledge helpful advice and review of drafts by Celgene and Agios colleagues, especially Krishnan Viswanadhan, Samantha Good, and Kyle Macbeth. We thank Sung Choe (Agios Pharmaceuticals) for helpful discussions, operational assistance and data cleaning.

Authorship Contributions and Disclosures: MA, LQ, AS, MR, BM and NFR performed experiments. ES, SB and MD coordinated sample collection. All authors contributed to experimental design, analyzed data and edited the manuscript. PV, RL and MA wrote the

manuscript. AT led all translational studies and analysis efforts. LQ was supported by a fellowship from Celgene. PV and LQ acknowledge funding from the MRC (MHU Award G1000729, MRC Disease Team Award 4050189188), CRUK (Program Grant to PV C7893/A12796, CRUK program grant to BG C1163/A21762), Bloodwise (Specialist Program 13001) and the Oxford Partnership Comprehensive Biomedical Research Centre (NIHR BRC Funding scheme). This work was supported by grant R01CA172636-01 to RLL, by grant U54OD020355-01 to RLL, by a supplement to P30CA008748 to RLL, and MSK cores used to perform studies included in this work are supported by P30CA008748. RLL is a scholar of the Leukemia and Lymphoma Society. AHS is supported by the Conquer Cancer Foundation and by NCIK08CA181507.

References

1. Gross S, Cairns RA, Minden MD, et al. Cancer-associated metabolite 2-hydroxyglutarate accumulates in acute myelogenous leukemia with isocitrate dehydrogenase 1 and 2 mutations. *J Exp Med*. 2010;207(2):339-344.
2. Ward PS, Patel J, Wise DR, et al. The common feature of leukemia-associated IDH1 and IDH2 mutations is a neomorphic enzyme activity converting alpha-ketoglutarate to 2-hydroxyglutarate. *Cancer Cell*. 2010;17(3):225-234.
3. Fathi AT, Sadrzadeh H, Borger DR, et al. Prospective serial evaluation of 2-hydroxyglutarate, during treatment of newly diagnosed acute myeloid leukemia, to assess disease activity and therapeutic response. *Blood*. 2012;120(23):4649-4652.
4. Janin M, Mylonas E, Saada V, et al. Serum 2-hydroxyglutarate production in IDH1- and IDH2-mutated de novo acute myeloid leukemia: a study by the Acute Leukemia French Association group. *J Clin Oncol*. 2014;32(4):297-305.
5. Xu W, Yang H, Liu Y, et al. Oncometabolite 2-hydroxyglutarate is a competitive inhibitor of alpha-ketoglutarate-dependent dioxygenases. *Cancer Cell*. 2011;19(1):17-30.
6. Lu C, Ward PS, Kapoor GS, et al. IDH mutation impairs histone demethylation and results in a block to cell differentiation. *Nature*. 2012;483(7390):474-478.
7. Figueroa ME, Abdel-Wahab O, Lu C, et al. Leukemic IDH1 and IDH2 mutations result in a hypermethylation phenotype, disrupt TET2 function, and impair hematopoietic differentiation. *Cancer Cell*. 2010;18(6):553-567.
8. Losman JA, Looper RE, Koivunen P, et al. (R)-2-hydroxyglutarate is sufficient to promote leukemogenesis and its effects are reversible. *Science*. 2013;339(6127):1621-1625.
9. Wang F, Travins J, DeLaBarre B, et al. Targeted inhibition of mutant IDH2 in leukemia cells induces cellular differentiation. *Science*. 2013;340(6132):622-626.
10. Kats LM, Reschke M, Taulli R, et al. Proto-oncogenic role of mutant IDH2 in leukemia initiation and maintenance. *Cell Stem Cell*. 2014;14(3):329-341.
11. Green CL, Evans CM, Zhao L, et al. The prognostic significance of IDH2 mutations in AML depends on the location of the mutation. *Blood*. 2011;118(2):409-412.
12. Molenaar RJ, Thota S, Nagata Y, et al. Clinical and biological implications of ancestral and non-ancestral IDH1 and IDH2 mutations in myeloid neoplasms. *Leukemia*. 2015;29(11):2134-2142.
13. Papaemmanuil E, Gerstung M, Bullinger L, et al. Genomic classification and prognosis in acute myeloid leukemia. *N Engl J Med*. 2016;374(23):2209-2221.
14. Yen K, Wang F, Travins J, et al. AG-221 Offers a survival advantage in a primary human IDH2 mutant AML xenograft model. *Blood* 2013;122:240.
15. Shih AH, Shank KR, Meydan C, et al. AG-221, a Small molecule mutant IDH2 inhibitor, remodels the epigenetic state of IDH2-mutant cells and induces alterations in self-renewal/differentiation in IDH2-mutant AML model in vivo. *Blood* 2014 124:437.
16. Quivoron C, David M, Straley K, et al. AG-221, an oral, selective, first-in-class, potent IDH2-R140Q mutant inhibitor, induces differentiation in a xenotransplant model. *Blood* 2014;124:3735.
17. Shih AH, Meydan C, Shank K, et al. Combination targeted therapy to disrupt aberrant oncogenic signaling and reverse epigenetic dysfunction in IDH2- and TET2-mutant acute myeloid leukemia. *Cancer Discov*. 2017.
18. Stein E, DiNardo C, Pollyea D, et al. Enasidenib in mutant-IDH2 relapsed or refractory acute myeloid leukemia. *Blood*. 2016;in press.
19. Walter RB, Gooley TA, Wood BL, et al. Impact of pretransplantation minimal residual disease, as detected by multiparametric flow cytometry, on outcome of myeloablative hematopoietic cell transplantation for acute myeloid leukemia. *J Clin Oncol*. 2011;29(9):1190-1197.
20. Walter RB, Gyurkocza B, Storer BE, et al. Comparison of minimal residual disease as outcome predictor for AML patients in first complete remission undergoing myeloablative or nonmyeloablative allogeneic hematopoietic cell transplantation. *Leukemia*. 2015;29(1):137-144.
21. He J, Abdel-Wahab O, Nahas MK, et al. Integrated genomic DNA/RNA profiling of hematologic malignancies in the clinical setting. *Blood*. 2016;127(24):3004-3014.
22. Fan B, Chen Y, Wang F, et al. Evaluation of pharmacokinetic-pharmacodynamic (PKPD) relationship of an oral, selective, first-in-class, potent IDH2 inhibitor, AG-221, from a Phase 1 trial in patients with advanced IDH2 mutant positive hematologic malignancies. *Blood*. 2014;124(21):3737.
23. Fan B, Chen Y, Wang F, et al. PHARMACOKINETIC/PHARMACODYNAMIC (PK/PD) EVALUATION OF AG-221, A POTENT MUTANT IDH2 INHIBITOR, FROM A PHASE 1 TRIAL OF PATIENTS WITH IDH2-MUTATION POSITIVE HEMATOLOGIC MALIGNANCIES. *Haematologica*. 2015;100 (1 Supplement):379.

24. Gao Y, Fan B, Le K, et al. Evaluation of the pharmacokinetics of AG-221, a potent mutant IDH2 inhibitor, in patients with IDH2-mutation positive advanced hematologic malignancies in a phase 1/2 trial. *Blood*. 2015;126(23):2509.
25. DiNardo C, de Botton S, Stein E, et al. Determination of IDH1 mutational burden and clearance via next-generation sequencing in patients with IDH1 mutation-positive hematologic malignancies receiving AG-120, a first-in-class inhibitor of mutant IDH1 *Blood*. 2016;128(22):1070.
26. Grimwade D, Ivey A, Huntly BJ. Molecular landscape of acute myeloid leukemia in younger adults and its clinical relevance. *Blood*. 2016;127(1):29-41.
27. Mrozek K, Marcucci G, Nicolet D, et al. Prognostic significance of the European LeukemiaNet standardized system for reporting cytogenetic and molecular alterations in adults with acute myeloid leukemia. *J Clin Oncol*. 2012;30(36):4515-4523.
28. Dohner H, Estey E, Grimwade D, et al. Diagnosis and management of AML in adults: 2017 ELN recommendations from an international expert panel. *Blood*. 2017;129(4):424-447.
29. Dohner H, Estey EH, Amadori S, et al. Diagnosis and management of acute myeloid leukemia in adults: recommendations from an international expert panel, on behalf of the European LeukemiaNet. *Blood*. 2010;115(3):453-474.
30. Goardon N, Marchi E, Atzberger A, et al. Coexistence of LMPP-like and GMP-like leukemia stem cells in acute myeloid leukemia. *Cancer Cell*. 2011;19(1):138-152.
31. Quek L, Otto GW, Garnett C, et al. Genetically distinct leukemic stem cells in human CD34- acute myeloid leukemia are arrested at a hemopoietic precursor-like stage. *J Exp Med*. 2016;213(8):1513-1535.
32. Stein E, DiNardo C, Altman J, et al. Safety and Efficacy of AG-221, a Potent Inhibitor of Mutant IDH2 That Promotes Differentiation of Myeloid Cells in Patients with Advanced Hematologic Malignancies: Results of a Phase 1/2 Trial. *Blood*. 2015;126(23):323.
33. Warrell RP, Jr., Frankel SR, Miller WH, Jr., et al. Differentiation therapy of acute promyelocytic leukemia with tretinoin (all-trans-retinoic acid). *N Engl J Med*. 1991;324(20):1385-1393.

Tables

Table 1: Analysis of Response in Patients with Favorable, Intermediate, and Adverse-Risk rrAML

Risk Assessment	ORR / CR, Favorable Risk Profile %, (n)	ORR / CR, Intermediate Risk (I+II) Profile %, (n)	ORR / CR, Adverse Risk Profile %, (n)	P-value (ORR / CR)
Risk Classification				
ELN 2010	22.2% / 0%, (9)	55.8% / 32.6%, (43)	30.0% / 10.0%, (20)	0.7322 / 0.8493
ELN 2017	37.5% / 0%, (8)	65.2% / 43.5%, (23)	34.1%/ 14.6% (41)	0.2049 / 0.5816
Grimwade	33.3% / 0%, (6)	66.7% / 58.3%, (12)	40.7% / 16.7%, (54)	0.6121 / 0.4487
Molecular Classification				
Papaemmanuil*	80.0% / 60.0%, (5)	36.4% / 9.0%, (11)	42.8% / 21.4%, (56)	0.4631 / 0.2605

ORR (CR, CRi, CRp, MLFS, and PR) by risk assessment based on cytogenetic testing and mutations identified by FoundationOne® Heme panel according to ELN 2010[29], ELN 2017[28], Grimwade et al.[26], and Papaemmanuil et al.[13] *Papaemmanuil risk was inferred from survival analysis of molecular classifications where m*CEBPA* and m*IDH2*-R172 groups were considered favorable, m*NPM1* and others were considered intermediate, and chromosome 3 inversion, Chromatin-Spliceosome, *MLL* fusions and m*TP53*-aneuploidy were considered adverse. P-value for contingency test for logical trend from favorable to adverse risk.

Figure Legends

Figure 1. mIDH2 Inhibition Is Associated with Potent Reduction of 2-HG in mIDH2 AML.

(A) Dot plot with median and interquartile range showing maximum 2-HG suppression (% change from baseline) in blood observed in patients segregated by R140 and R172 mIDH2. Numbers indicate number of patients from each genotype graphed.

(B) Dot plot with median and interquartile range showing maximum 2-HG suppression (% change from baseline) observed in patients segregated by total daily dose received (<100 mg in green, 100mg in blue, >100 mg in purple) and stratified by R140 and R172 mIDH2.

(C) Dot plot with median and interquartile range showing blood plasma 2-HG (ng/ml) at screening in patients segregated by best response achieved and stratified by R172 (red) and R140 (blue) mIDH2. Response (R) is defined as either complete remission (CR), CR with incomplete count recovery (CRi), CR with incomplete platelet count recovery (CRp), morphologic leukemia-free state (MLFS) or partial remission (PR). No response (NR) is defined as stable disease (SD) or progressive disease (PD).

(D) Whisker plot indicating mean and standard deviation of cycle to CR, Best Response (BR) or maximum 2-HG suppression (Max 2-HG) stratified by R172 (red) and R140 (blue) mIDH2.

Figure 2. Clinical Responses to mIDH2 Inhibition Do Not Correlate with m*IDH2* Allele Burden

(A) Dot plot of m*IDH2* variant allele frequency (VAF) (R140 mIDH2 in blue and R172 mIDH2 in red) in patient samples measured at screening in either peripheral blood (PB) or bone marrow (BM) by FoundationOne® Heme panel. Measurements separated by the best response achieved by patients, as defined in Figure 1. Numbers indicate the number of patient samples in the graph.

(B) Waterfall plot indicating absolute change in m*IDH2* VAF from screening to achievement of best response measured by Sysmex OncoBeam digital PCR. Responders in green and non-responders in red. Patients achieving CR are outlined in black. The dotted line indicates the largest VAF decrease observed in a non-responder.

(C) Line graph of m*IDH* VAF over time (days of treatment) in 9 patients achieving molecular remission (undectable m*IDH2*) for at least one time point during treatment.

(D) Scatter plot of bone marrow m*IDH2* VAF vs blast percentage measured by flow cytometry in nine responsive patients in samples taken pre-treatment (pre-Rx: red) and at response (CR, CRi, CRp or MLFS; green). Blue line indicates expected ratio (2:1) between blast percent:m*IDH2* VAF in clonal m*IDH2* disease. Three data points (in green) are superimposed with values close to or at 0.

Figure 3. Clinical Response to mIDH2 Inhibition Is Associated with Induction of Myeloid Differentiation

(A) Representative immunophenotypic analyses by flow cytometry on sequential bone marrow samples. Cell-surface markers studied are shown. Left, data from a responding patient (pre-treatment [Pre] to complete remission (CR) to relapse). Right, data from a non-responding patient (pre-treatment to progressive disease [PD]) who remained in stable disease during treatment. Numbers in FACS plots refer to size of the population as a percentage of lineage-negative bone marrow mononuclear cells. For normal bone marrow (n=12) standard deviation of ±2.7% for immature progenitor, ±9.6% for immature precursors, and ±9.7% for mature myeloid cells.

(B) Top, Graph showing ratio of immature to mature cell populations by flow cytometry from bone marrow over time: The average ratios of myeloid progenitor or myeloid precursors to mature myeloid cells in bone marrow from normal donors (n=12) and 5 patients who either had a CR or PR with enasidenib are shown. In patient 201-010, the changing size of myeloid precursor (red) cell populations relative to mature myeloid cells shown. In the remaining 3 patients, the changing size of myeloid progenitor (blue) populations to mature cells is shown. Colored bars represent the 95% confidence interval in normal controls. Bottom, the m*IDH2* VAF in each patient at different time points in all bone marrow mononuclear cells (VAF total) and in FACS-sorted mature myeloid cells ($CD34^{-}CD117^{-}$).

(C) Top, mIDH2 VAF in bone marrow mononuclear cells prior to treatment (Pre, blue) and in sorted peripheral blood neutrophils at time of best response (Post, red) in seven patients achieving CR. Middle and Bottom, VAF of indicated mutation in bone marrow mononuclear cells prior to treatment and in sorted peripheral blood neutrophils at time of best response in two patients achieving CR.

(D) Histogram of the percentages of functional neutrophils observed in *ex-vivo* enasidenib-treated patient samples (left) and representative images (right) assessed by phagocytic assay quantifying neutrophils (blue) that contained latex beads (green). The percentage of neutrophils containing beads was measured by scoring five different fields of view per sample.

Figure 4. Association of Co-occurring Mutations with Clinical Response and Classification of Patients from Cytogenetic and Molecular Abnormalities

(A) Tile plot showing the number of co-occurring somatic mutations by gene identified in FoundationOne® Heme panel from efficacy-evaluable patients separated by R140 and R172 m*IDH2*. Only mutated genes occurring in two or more patients are shown. Mutations associated with higher risk are in red and mutations associated with lower risk are in green, as defined by Grimwade, et al.[26]

(B) Histogram of the number of mutations identified in each gene from all 100 patient samples analyzed. Number of mutations identified in responding patients in blue, number of mutations identified in non-responding patients in red, and number of mutations in patients who were not efficacy evaluable in grey.

(C) Pie charts of proportions of patients in various risk categories according to European LeukemiaNet (ELN) 2010 AML risk stratification,[29] ELN 2017 AML risk stratification,[28] and

Grimwade et al.,[26] based on cytogenetic testing completed before start of Cycle 2 and mutations identified at screening.

(D) Pie chart of proportions of patients in various genomic classifications according to Papaemmanuil et al.,[13] based on cytogenetic testing completed before start of Cycle 2 and mutations identified at screening.

Figure 5. Co-mutational Burden and *NRAS* Mutations Are Associated with Lack of Response

(A) Scatter plot showing mean and standard deviation of number of mutations found per patient, separated by response. P-value < 0.001 comparing difference between non-responders (NR) and either responders (R: CRi, CRp, MLFS, or PR) or patients achieving a CR.

(B) Pie charts of response assessment and overall response rate (ORR; patients achieving CR, CRi, CRp, MLFS or PR) in patients with the lowest third number of co-mutations (≤3 mutations) and highest third (≥6 mutations).

(C) Pie chart indicating proportion of responders and non-responders in the 14 efficacy evaluable patients with *NRAS* co-mutations (m*NRAS*), specifically at G12, G13, and Q61.

(D) Number of mutations found per patient separated by presence of G12, G13, or Q61 mutant m*NRAS* indicating patients with m*NRAS* at G12, G13, or Q61 have increased mutational burden in this cohort. The only m*NRAS*+ patient to achieve a CR is highlighted in green.

(E) Dot plot of m*IDH2* (blue) and m*NRAS* (red) VAF in same patient in the 14 efficacy evaluable patients with *NRAS* co-mutations specifically at G12, G13, and Q61. R = responder, NR = non-responder.

Figure 1.

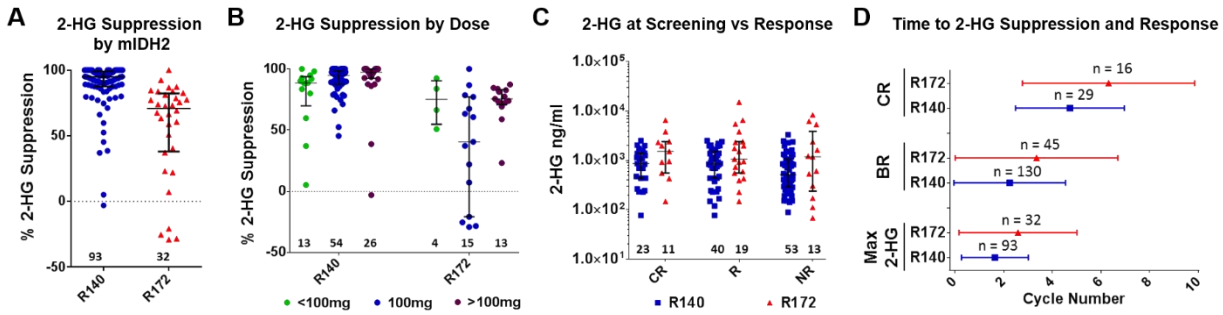
A
2-HG Suppression by mIDH2
% 2-HG Suppression
100
50
0
-50
93
32
R140
R172
B
2-HG Suppression by Dose
% 2-HG Suppression
100
50
0
-50
13
54
26
4
15
13
R140
R172
<100mg
100mg
>100mg
C
2-HG at Screening vs Response
2-HG ng/ml
1.0×10⁵
1.0×10⁴
1.0×10³
1.0×10²
1.0×10¹
23
11
40
19
53
13
CR
R
NR
R140
R172
D
Time to 2-HG Suppression and Response
CR
BR
Max 2-HG
R172
R140
n = 16
n = 29
n = 45
n = 130
n = 32
n = 93
0
2
4
6
8
10
Cycle Number

Figure 2.

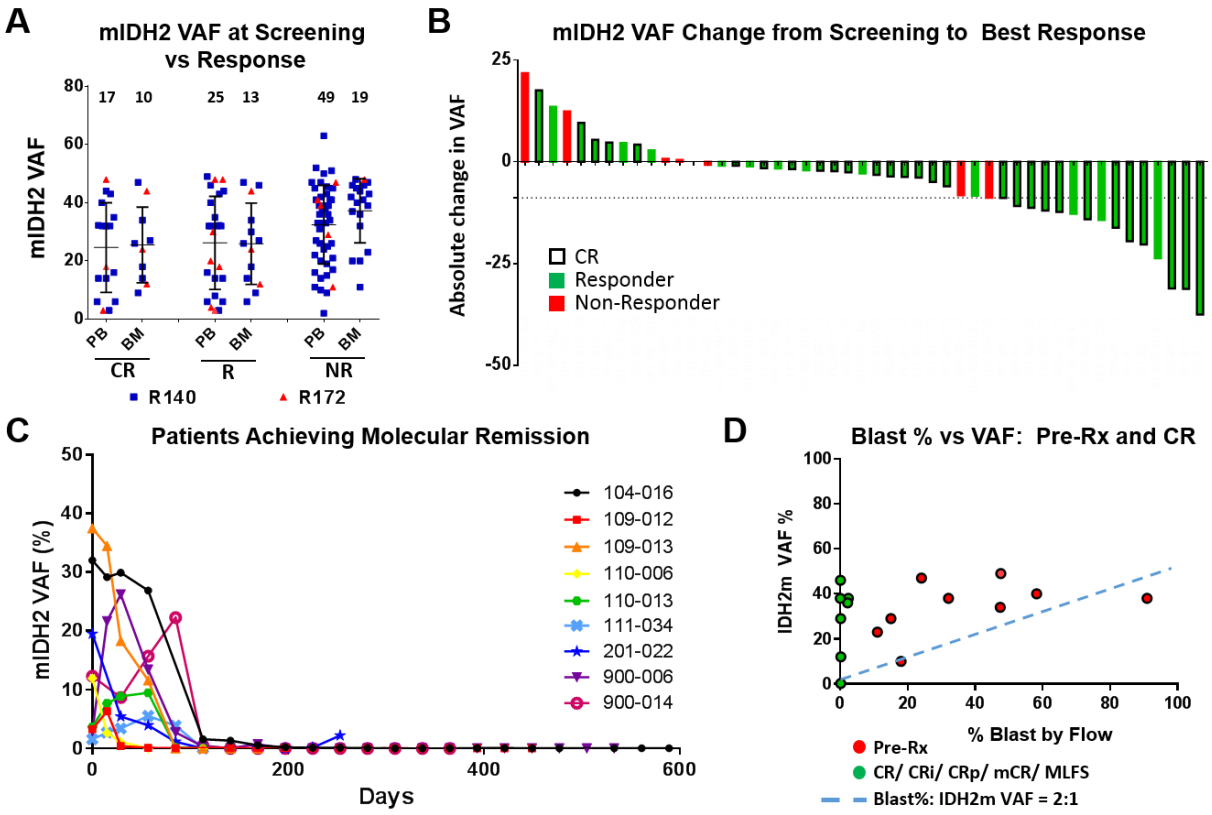
A
mIDH2 VAF at Screening vs Response
mIDH2 VAF
17 10 25 13 49 19
PB BM PB BM PB BM
CR R NR
R140 R172
B
mIDH2 VAF Change from Screening to Best Response
Absolute change in VAF
CR
Responder
Non-Responder
C
Patients Achieving Molecular Remission
mIDH2 VAF (%)
Days
104-016
109-012
109-013
110-006
110-013
111-034
201-022
900-006
900-014
D
Blast % vs VAF: Pre-Rx and CR
IDH2m VAF %
% Blast by Flow
Pre-Rx
CR/ CRi/ CRp/ mCR/ MLFS
Blast%: IDH2m VAF = 2:1

Figure 3.

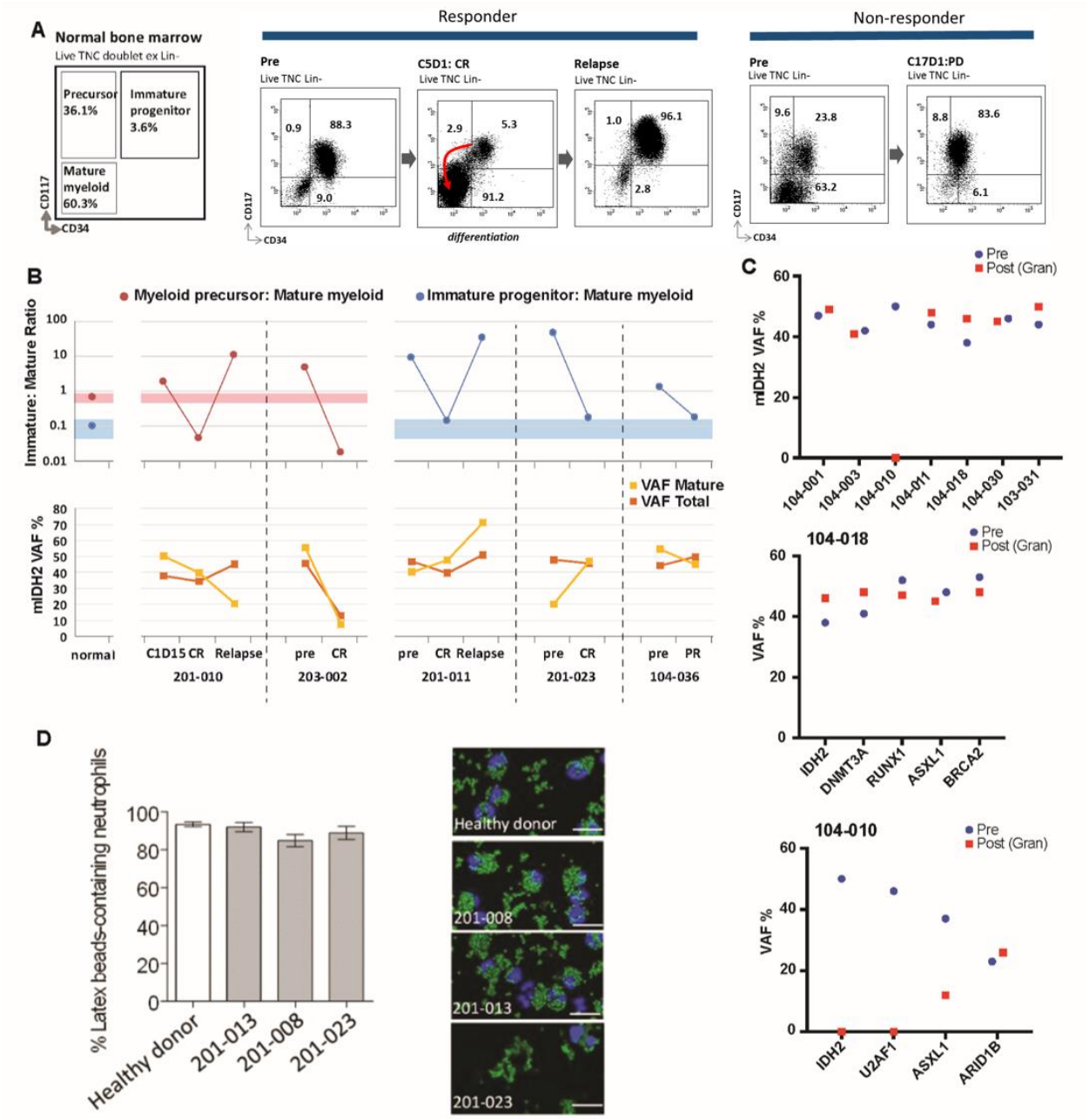
A
Normal bone marrow
Live TNC doublet ex Lin-
Precursor 36.1%
Immature progenitor 3.6%
Mature myeloid 60.3%
CD117
CD34
Responder
Non-responder
Pre
Live TNC Lin-
C5D1: CR
Relapse
C17D1:PD
0.9
88.3
9.0
2.9
5.3
91.2
1.0
96.1
2.8
9.6
23.8
63.2
8.8
83.6
6.1
differentiation
B
Myeloid precursor: Mature myeloid
Immature progenitor: Mature myeloid
Immature: Mature Ratio
mIDH2 VAF %
VAF Mature
VAF Total
normal
C1D15 CR
Relapse
pre
CR
201-010
203-002
201-011
201-023
104-036
PR
C
Pre
Post (Gran)
mIDH2 VAF %
104-001
104-003
104-010
104-011
104-018
104-030
103-031
104-018
VAF %
IDH2
DNMT3A
RUNX1
ASXL1
BRCA2
104-010
U2AF1
ARID1B
D
% Latex beads-containing neutrophils
Healthy donor
201-013
201-008
201-023

Figure 4.

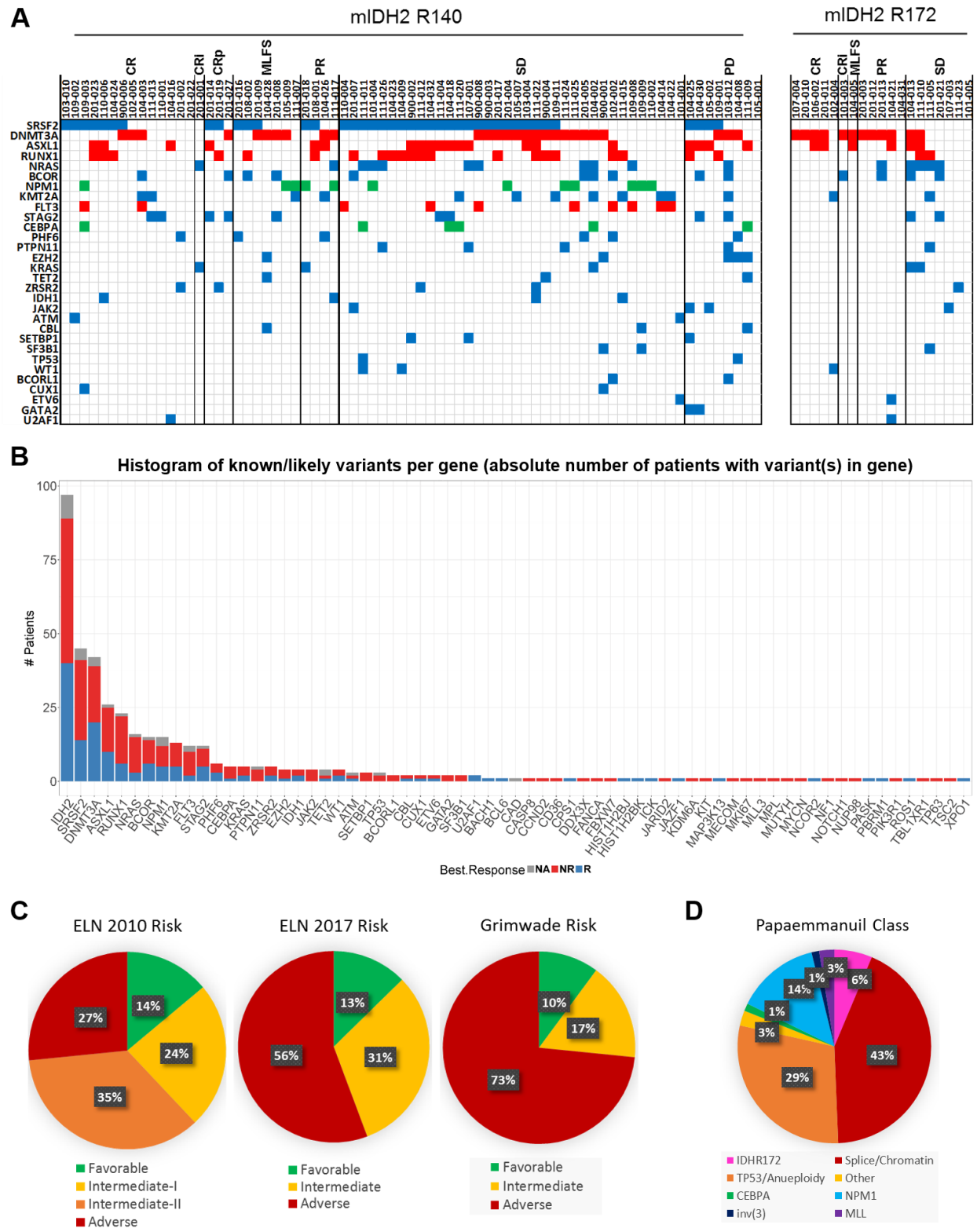
A
mIDH2 R140
mIDH2 R172
CR
CRi
CRp
MLFS
PR
SD
PD
SRSF2
DNMT3A
ASXL1
RUNX1
NRAS
BCOR
NPM1
KMT2A
FLT3
STAG2
CEBPA
PHF6
PTPN11
EZH2
KRAS
TET2
ZRSR2
IDH1
JAK2
ATM
CBL
SETBP1
SF3B1
TP53
WT1
BCORL1
CUX1
ETV6
GATA2
U2AF1
B
Histogram of known/likely variants per gene (absolute number of patients with variant(s) in gene)
Patients
Best.Response NA NR R
C
ELN 2010 Risk
14%
24%
35%
27%
Favorable
Intermediate-I
Intermediate-II
Adverse
ELN 2017 Risk
13%
31%
56%
Favorable
Intermediate
Adverse
Grimwade Risk
10%
17%
73%
Favorable
Intermediate
Adverse
D
Papaemmanuil Class
6%
43%
29%
3%
1%
14%
1%
3%
IDHR172
Splice/Chromatin
TP53/Anueploidy
Other
CEBPA
NPM1
inv(3)
MLL

Figure 5.

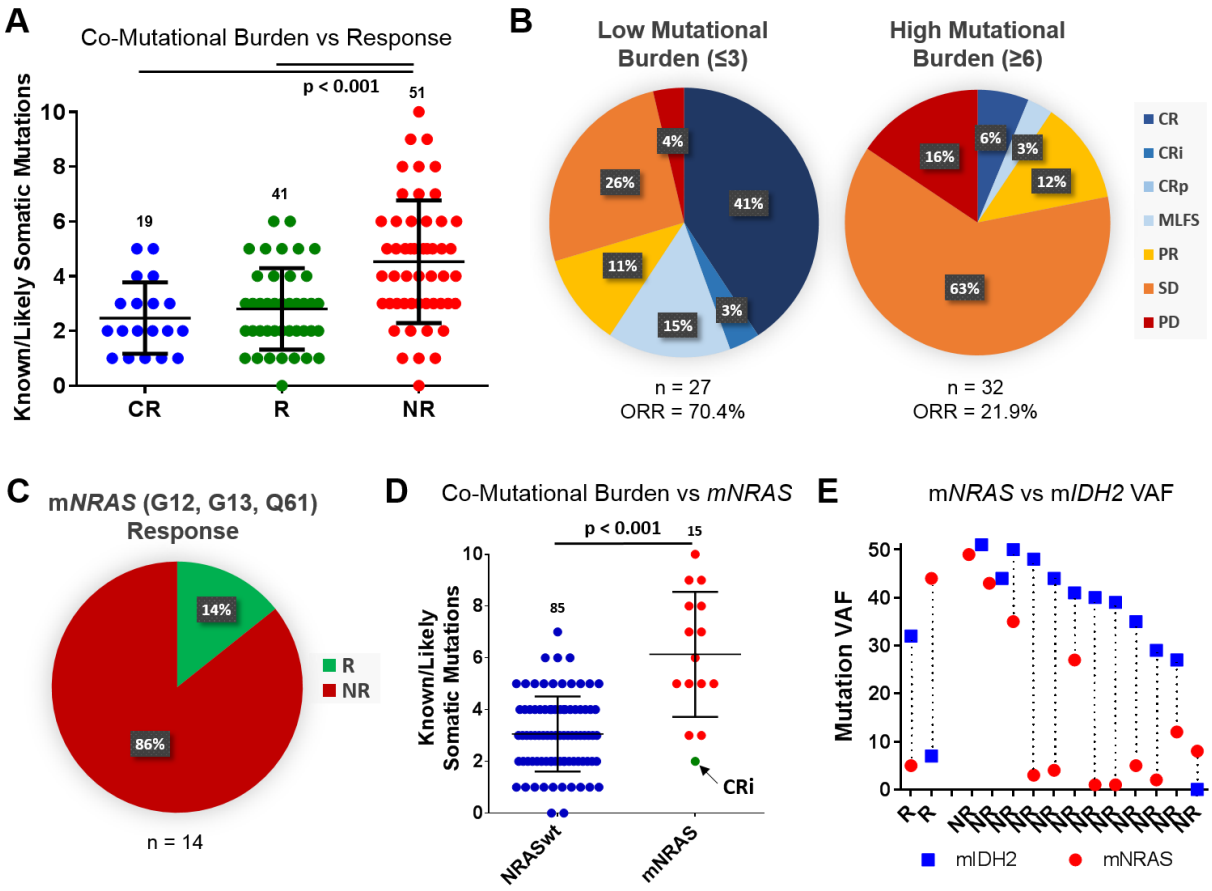
A
Co-Mutational Burden vs Response
p < 0.001
Known/Likely Somatic Mutations
CR
R
NR
19
41
51
B
Low Mutational Burden (≤3)
High Mutational Burden (≥6)
CR
CRi
CRp
MLFS
PR
SD
PD
n = 27
ORR = 70.4%
n = 32
ORR = 21.9%
C
mNRAS (G12, G13, Q61) Response
R
NR
n = 14
D
Co-Mutational Burden vs mNRAS
p < 0.001
Known/Likely Somatic Mutations
NRASwt
mNRAS
CRi
E
mNRAS vs mIDH2 VAF
Mutation VAF
mIDH2
mNRAS

Supplementary Materials

Figure S1

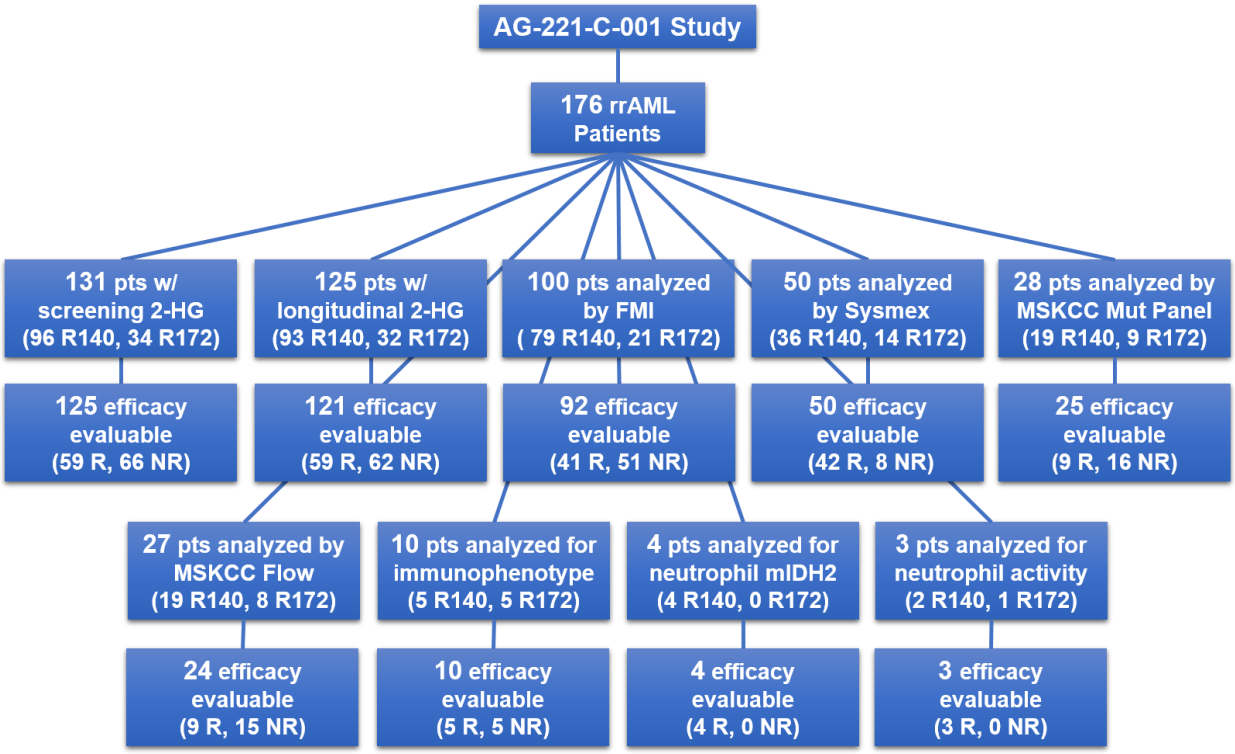

Figure S1: Patient Sample Availability and Analysis Disposition

Patient sample disposition indicating of 176 rrAML patients from the AG-221-C-001 study; i.e., the sample availability for each assay. Of available samples, only a subset had clinical efficacy data, defined as those patients who received enasidenib and an investigator-assessed clinical response was captured from at least one time-point during treatment. Number of samples from patients with R140 vs R172 m*IDH2* and from patients achieving a response (R) vs no response (NR) (as defined in Figure 1) are indicated. rrAML, relapsed/refractory acute myeloid leukemia, FMI, Foundation Medicine, Inc. FoundationOne® Heme Assay. MSKCC, Memorial Sloan Kettering Cancer Center.

Figure S2

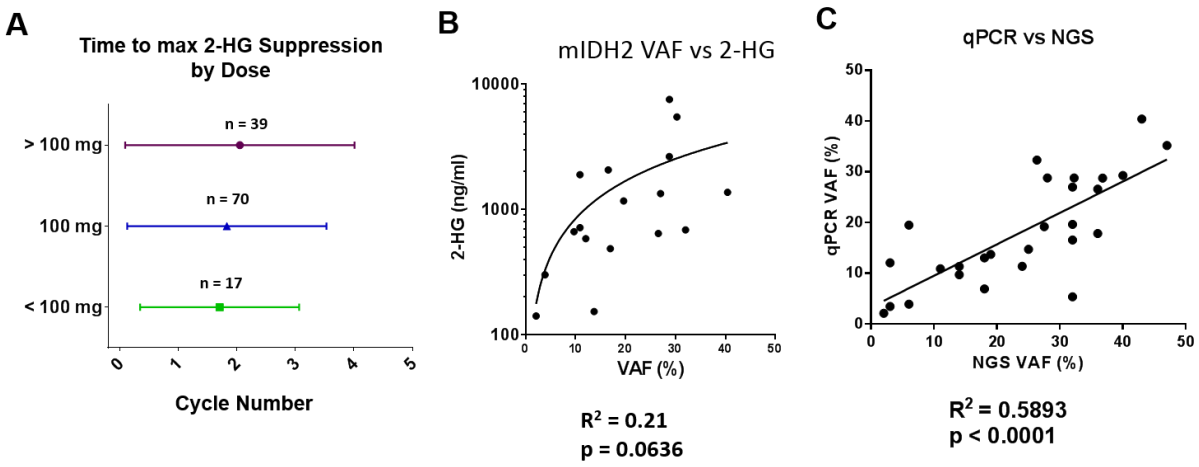

Figure S2. Analysis of 2-HG and mIDH2 Variant Allele Frequency

A. Whisker plot indicating mean and standard deviation of cycle to maximum 2-HG suppression (Max 2-HG) stratified by patients dosed with <100mg, 100mg, or >100mg enasidenib daily.

B. Scatter plot and regression analysis of m*IDH2* variant allele frequency (VAF) in patient samples at screening analyzed by Sysmex OncoBeam digital PCR assay with levels of 2-HG in plasma in the same patient (n=17).

C. Scatter plot and regression analysis of m*IDH2* VAF in patient samples when VAF was measured in the same patient at the same time point by both an NGS panel (either FoundationOne® Heme, n=26, or MSKCC panel, n=3, as discussed in Methods) and Sysmex OncoBeam digital PCR assay.

Figure S3

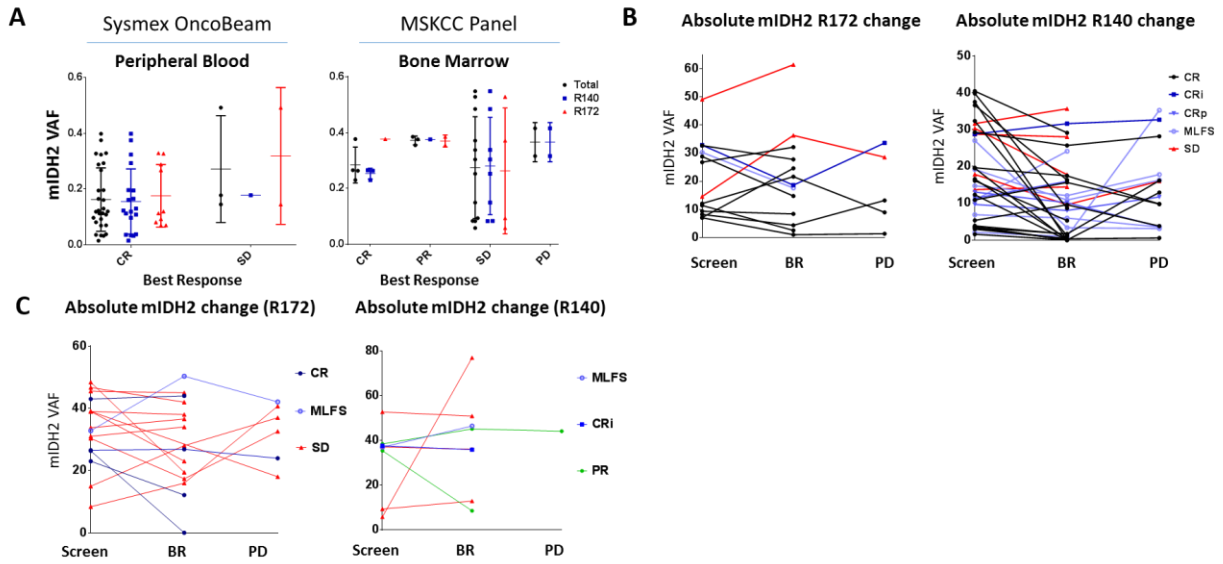

Figure S3. mIDH2 Variant Allele Frequency and Response

A. Dot plot of m*IDH2* VAF in patient samples measured by Sysmex digital PCR (left) or Memorial Sloan Kettering Cancer Center (MSKCC) mutational panel (right) at screening. Measurements were separated by best response (BR) achieved by the patient (CR, CRp, CRi, or MLFS) and m*IDH2* status (red = R140, blue = R172, black = combined).

B. Scatter plots of m*IDH2* VAF level measured by Sysmex digital PCR in R172 (left) and R140 (right) m*IDH2* patients. Lines indicate changes in m*IDH2* levels in individual patients from screening to first achievement of BR to disease progression (PD, if available). Black lines indicate patients' BR of CR, blue lines indicate BR of CRi, CRp, or MLFS, and red lines indicate BR of SD (SD patients' samples were analyzed at Cycle 3 Day 1).

C. Scatter plots of mIDH2 VAF level measured by NGS panels in mIDH2 R172 (left) and R140 (right) patients. Lines indicate changes in m*IDH2* levels in individual patients from screening to first achievement of BR and then to PD (if available). Black lines indicate patients' BR of CR, blue lines indicate BR of CRi or MLFS, green lines indicate BR of PR, and red lines indicate BR of SD (SD patients' samples were analyzed at Cycle 3 Day 1).

Figure S4

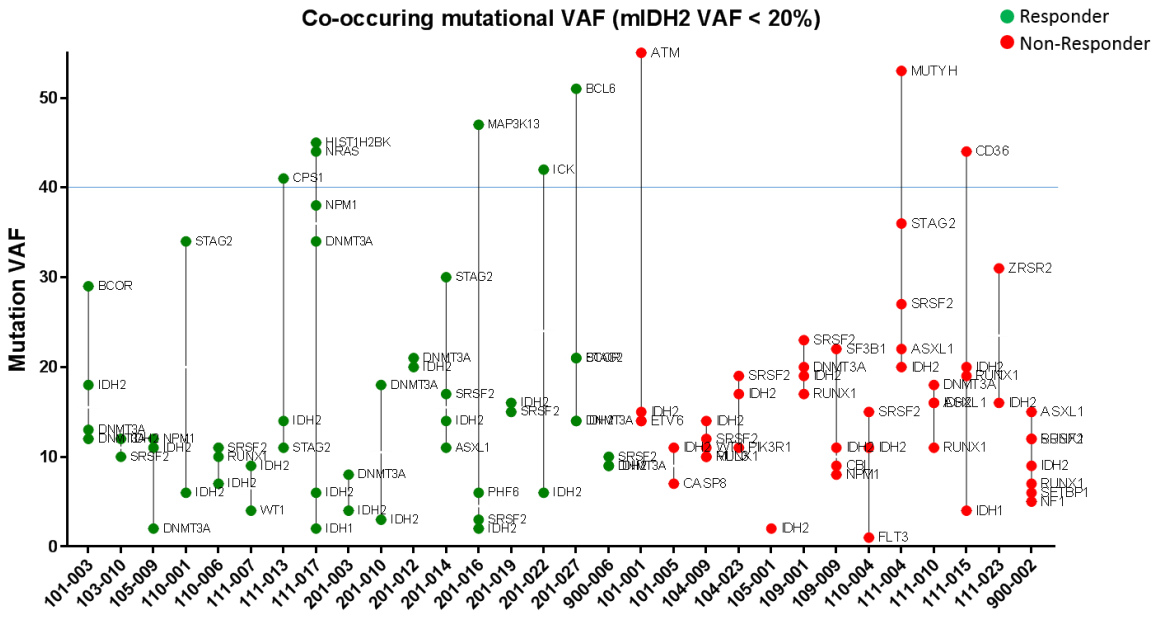

Figure S4: VAF of co-occurring mutations in patients with low mIDH2

Co-mutational variant allele frequency (VAF) measured by FoundationOne® Heme panel in individual patients with subclonal mIDH2 (VAF <20%). Responding patients (CR, CRi, CRp, MLFS, or PR) in green, non-responding patients (SD or PD) in red.

Figure S5

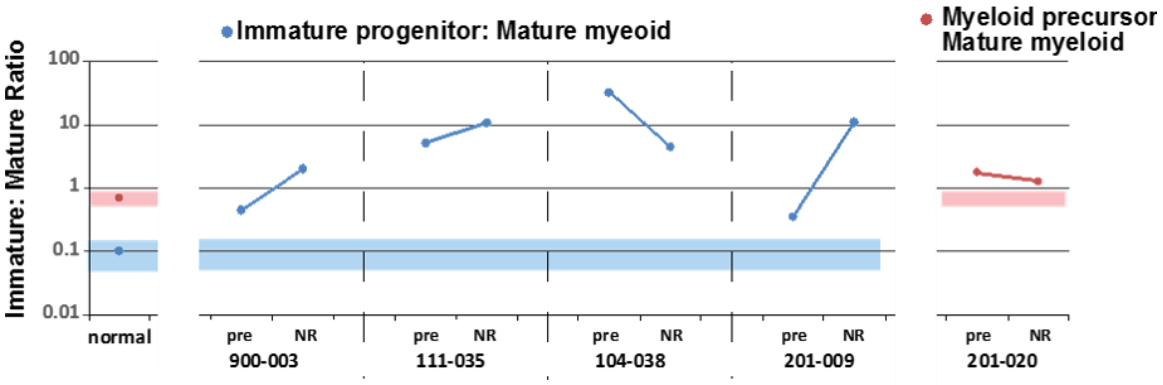

Figure S5. Mature and Immature Cell Populations from Bone Marrow in Non-Responding Patients

Graph showing ratio of immature to mature cell populations from bone marrow: The average ratios of myeloid progenitor or myeloid precursors to mature myeloid cells in bone marrow from normal donors (n=12) are shown. Colored bars represent the 95% confidence interval. The same analysis was applied to samples from four non-responding patients with expanded leukemic myeloid progenitors and one patient (201-020) who had expanded leukemic myeloid precursors.

Figure S6

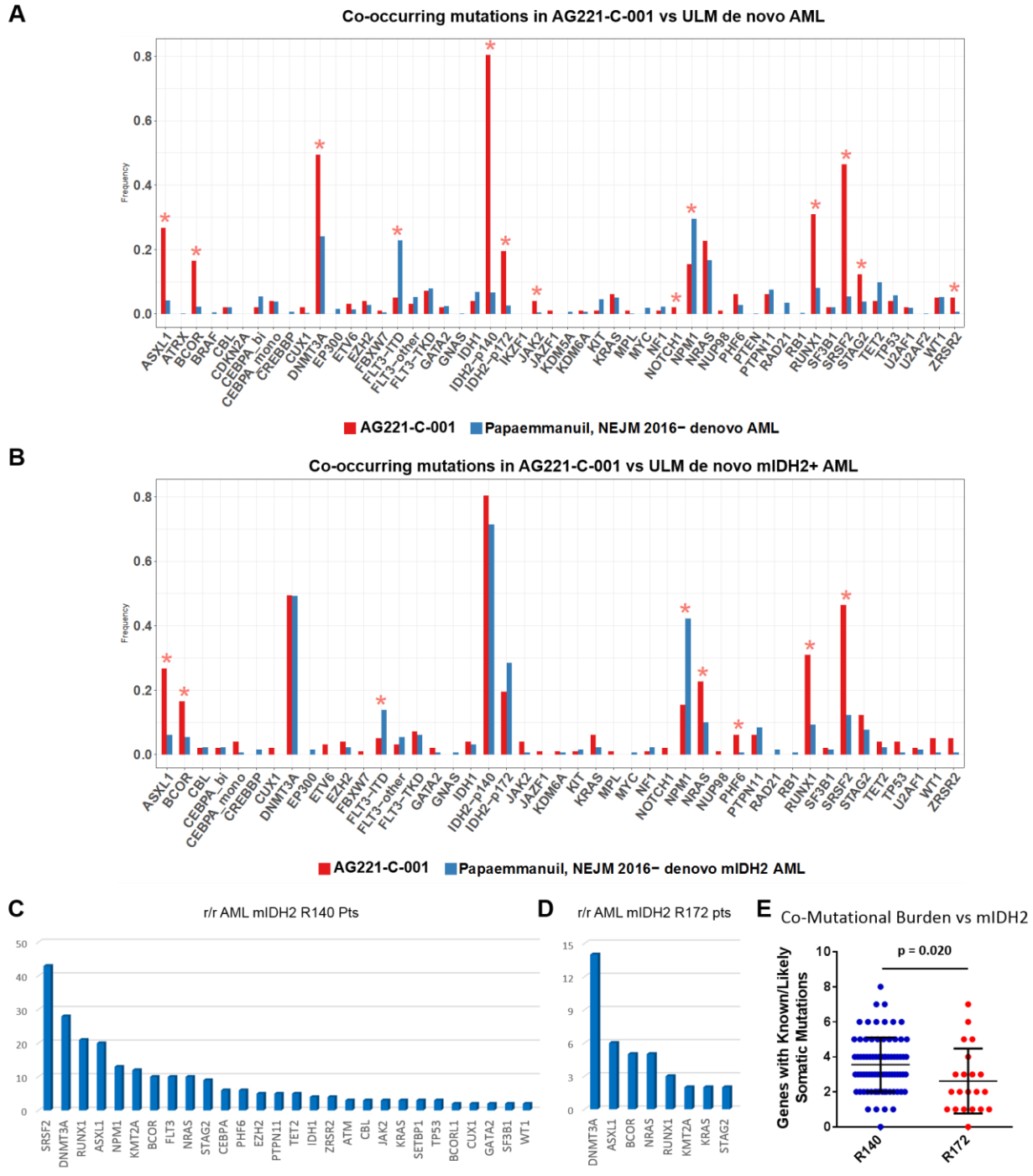

Figure S6: Co-occurring Mutation Frequency vs Response

A. Comparison of co-occurring mutation frequency in AG-221-C-001 (red) vs the same mutations in all 1376 cases of de novo AML from Papaemmanuil, et al (blue).[13] Genes

that were not part of the Papaemmanuil, et al. dataset or FoundationOne® Heme panel were removed. Fisher Exact Test was used to compare gene counts between datasets. * indicates significant enrichment of gene in either data set (p-value ≤ 0.05).

B. Comparison of co-occurring mutation frequency in AG-221-C-001 (red) vs same co-occurring mutations in all 130 cases of de novo AML from Papaemmanuil, et al that were mIDH2 positive (blue).[13] Genes that were not part of the ULM dataset or FoundationOne® Heme panel were removed. Fisher Exact Test was used to compare gene counts between datasets. * indicates significant enrichment of gene in either data set (p-value ≤ 0.05).

C. Histogram of mutation frequency in genes found by FoundationOne® Heme panel in R140 m*IDH2* patients.

D. Histogram of mutation frequency in genes found by FoundationOne® Heme panel in R172 m*IDH2* patients.

E. Number of mutations found per patient separated by patients with m*IDH2* R140 vs R172. Hashes represent mean with standard deviation, p-value from student's t-test.

Table S1. Patient baseline characteristics in all relapsed/refractory AML patients from the AG221-C-001 trial and patient subgroup analyzed.

	FoundationOne® Patients n=100	Sysmex mIDH2 VAF Patients n=50	2-HG Patients N= 125	All R/R AML Patients n=176
ORR (%)	41.0	84.0	47.2	40.3
CR (%)	19.0	60.0	20.8	19.3
Median Age, years	65.7	67.6	65.2	65.2
Sex M/F (%)	51.0/49.0	36.0/64.0	52.0/48.0	51.1/48.9
Gene Mutation (%): R140/R172	79.0/21.0	74.0/26.0	74.4/26.6	73.9/25.6
No. of Prior Anticancer therapies (%): 1/2/3/4/>=5	46.0/23.0/16.0/ 11.0/4.0	56.0/26.0/6.0/ 10.0/2.0	50.4/22.4/12.8/ 10.4/4.0	46.6/26.1/14.2/ 8.5/4.5
Prior Transplant (%)	14.0	16.0	14.4	13.6
Mean Bone Marrow Blast (%)	49.9	36.4	47.1	49.4
Mean ANC ($x10^9$/L)	1.5	1.6	1.3	1.3
Prior MDS (%)	16.0	10.0	16.0	17.0

Overall Response Rate (ORR) and Complete Remission (CR) rate and baseline characteristics, including age, sex (male/female), *IDH2* mutation subtype, number of prior anticancer therapies, patients who have received a transplant, baseline bone marrow blast percentage, mean absolute neutrophil count (ANC) and patients with prior diagnosis of MDS in the rrAML cohort in the AG-221-C-001 and in patient subgroups analyzed by FoundationOne® Heme mutation panel, Sysmex mIDH2 VAF digital PCR, and 2-HG assay.

Table S2. Multi-parameter Flow Cytometry (MFC) Ten-"Color" Panel.

Myeloid tube 1	Myeloid tube 2	Myeloid tube 3
CD15 FITC	CD64 FITC	CD7 BB515
CD33 PE	CD123 PE	CD56 PE
CD117 PC5	CD14 PC5	CD5 PerCP-Cy5.5
CD13 PE-CY7	CD13 PE-CY7	CD33 PE-CY7
CD34 APC	CD34 APC	CD34 APC
CD71 APC ALEXA700	CD16 APC ALEXA700	CD4 APC-ALEXA700
CD38 APC ALEXA 750	CD38 APC ALEXA750	CD38 APC-ALEXA750
HLA-DR PAC BLUE	HLA-DR PAC BLUE	CD2 BV421
CD45 V500C	CD45 V500C	CD45 V500c
CD19 BV605	CD11b BV605	CD25 BV605

Table S3. Antibody List Used for Hematopoietic Stem, Progenitor, and Mature Cell Population Immunophenotyping

Antigen	Clone	Fluorochrome	Source
CD10	eBIOCB-CALLA	None	Ebioscience, UK
CD117	104D2	PE	Biolegend, UK
CD11b	ICRF44	APC	Ebioscience, UK
CD19	HIB19	none	Ebioscience, UK
CD2	RPA-2.10	none	Ebioscience, UK
CD20	2H7	none	Ebioscience, UK
CD235a	HIR2	none	Ebioscience, UK
CD3	HIT3a	none	Ebioscience, UK
CD34	561	BV421	Biolegend, UK
CD4	RPA-T4	none	Ebioscience, UK
CD8a	RPA-T8	none	Ebioscience, UK
goat F(ab')2 anti-mouse secondary		QDOT605	Invitrogen
Streptavidin		APC EFluor780	Ebioscience, UK

Table S4. **Detection of *IDH2* Mutation in Peripheral Blood Neutrophils and Monocytes in Four Patients Treated with Enasidenib**

Patient	**Time point**	**Response**	**Mature cells analysed**	**m*IDH2* detected**
201-001	C1D8	NA	Neutrophil-enriched	yes
201-001	C2D1	MLFS	Neutrophil-enriched	yes
201-001	C3D1	CRi	Neutrophil-enriched	yes
201-001	C4D1	CRi	Neutrophil-enriched	yes
201-001	C4D8	NA	Neutrophil-enriched	yes
-	-	-	-	-
201-002	pre-treatment	NA	Neutrophil-enriched	yes
201-002	C1D8	NA	Neutrophil-enriched	yes
201-002	C1D15	CR	Neutrophil-enriched	yes
201-002	C1D18	CR	Neutrophil-enriched	yes
201-002	C1D25	CR	Neutrophil-enriched	yes
201-002	C2D1	CR	Neutrophil-enriched	yes
201-002	C2D15	CR	Neutrophil-enriched	yes
201-002	C2D22	CR	Neutrophil-enriched	yes
201-002	C3D1	CR	Neutrophil-enriched	yes
201-002	C3D4	CR	Neutrophil-enriched	yes
201-002	C3D8	CR	Neutrophil-enriched	yes

201-002	C3D22	CR	Neutrophil-enriched	yes
201-002	C4D1	CR	Neutrophil-enriched	yes
-	-	-	-	-
201-006	pre-treatment	NA	Neutrophil-enriched	yes
201-006	C1D15	CR	Neutrophil-enriched	yes
-	-	-	-	-
201-023	C1D8	NA	CD14+ monocytes	yes
201-023	C1D8	NA	CD16+ neutrophils	yes
201-023	C6D1	NA	CD14+ monocytes	yes
201-023	C6D1	NA	CD16+ neutrophils	yes
201-023	C8D15	CR	CD14+ monocytes	Yes

ANC = absolute neutrophil count; CR = complete remission; m*IDH2* = mutant *isocitrate dehydrogenase 2*

Mature neutrophils and monocytes isolated from longitudinal peripheral blood samples of enasidenib-treated patients were analyzed for the presence of *IDH2* mutation (R140Q or in sample 201-013: R172K) by TaqMan SNP genotyping. Samples were CD14+ monocytes and CD16+ neutrophils. C*n*D*n* denotes the cycle number and the day of the cycle the sample was obtained. Response assessments were made on D1 of each cycle, except for an additional early assessment at C1D15. Blood samples taken between response assessments are assigned the response at the previous cycle. NA denotes time points when response assessment was not available.

Table S5: Association of Known Somatic Mutations Identified by FoundationOne® Heme Panel with Response to Enasidenib.

Gene	R140 (n)	R172 (n)	ORR	ORR, OR	ORR, p-value	CR	CR, OR	CR, p-value
NRAS	12	5	0.188	0.275	0.0604	0.063	0.102	0.0114
PTPN11	5	1	0.000	0.114	0.0708	0.000	0.151	0.1598
RUNX1	21	3	0.261	0.418	0.1110	0.217	0.439	0.1609
JAK2	3	1	0.000	0.141	0.1351	0.000	0.186	0.2976
FLT3	11	1	0.200	0.312	0.1901	0.200	0.418	0.3300
SRSF2	45	0	0.341	0.610	0.2067	0.293	0.655	0.3498
ASXL1	21	6	0.385	0.799	0.6703	0.269	0.598	0.3750
CEBPA	6	0	0.167	0.254	0.2378	0.167	0.339	0.4181
STAG2	10	2	0.455	1.111	0.9999	0.455	1.500	0.5307
GATA2	2	0	0.000	0.507	0.2587	0.000	0.342	0.5344
BCORL1	2	0	0.000	0.574	0.5067	0.000	0.342	0.5344
TP53	3	0	0.000	0.259	0.5067	0.000	0.342	0.5344
ETV6	1	1	0.500	1.329	0.9999	0.000	0.342	0.5344
NPM1	15	0	0.417	0.942	0.9999	0.250	0.561	0.5388
SETBP1	3	0	0.000	0.183	0.2601	0.000	0.242	0.5544
SF3B1	2	1	0.000	0.183	0.2601	0.000	0.242	0.5544
EZH2	5	0	0.200	0.321	0.3920	0.200	0.542	0.6539
KRAS	3	2	0.400	0.879	0.9999	0.200	0.428	0.6539
KMT2A	12	2	0.357	0.716	0.7789	0.286	0.679	0.7724

U2AF1	1	1	1.000	6.799	0.1837	0.500	1.763	0.9999
DNMT3A	28	14	0.513	1.548	0.2689	0.359	0.974	0.9999
ATM	3	0	0.500	1.164	0.9999	0.500	1.763	0.9999
BCOR	10	5	0.429	0.996	0.9999	0.357	0.970	0.9999
CBL	3	0	0.333	0.657	0.9999	0.333	0.873	0.9999
CUX1	2	0	0.500	1.329	0.9999	0.500	1.763	0.9999
IDH1	4	0	0.500	1.333	0.9999	0.250	0.576	0.9999
PHF6	6	0	0.500	1.338	0.9999	0.333	0.871	0.9999
TET2	5	0	0.333	0.657	0.9999	0.333	0.873	0.9999
WT1	2	1	0.333	0.657	0.9999	0.333	0.873	0.9999
ZRSR2	4	1	0.400	0.879	0.9999	0.400	1.172	0.9999
CR = complete remission; ORR = overall response rate; OR = odds ratio								

Genes with known and likely somatic mutations identified by FoundationOne® Heme panel found in 2 or more patient samples sorted by p-value (Fisher's Exact test on contingency table). Overall response rates include CR, CRi, CRp, MLFS, or PR. CR rates include CR, CRi, CRp and MLFS.